

Optimization of glass-forming ability and synergistic enhancement of strength plasticity in $Cu_{50}Zr_{46}Al_4$ metallic glasses through Ag additions

Dongmei Li(李冬梅), Zhongyi Zhang(张忠一), Bolin Shang(尚博林), Rui Feng(丰睿), Xuefeng Li(李雪枫), and Peng Yu(余鹏)

Citation: Chin. Phys. B, 2025, 34 (**8**): 086107. DOI: 10.1088/1674-1056/adcea1
http://cpb.iphy.ac.cn; http://iopscience.iop.org/cpb

What follows is a list of articles you may be interested in

Atomic origin of minor alloying element effect on glass forming ability of metallic glass

Shan Zhang(张珊), Qingan Li(李庆安), Yong Yang(杨勇), and Pengfei Guan(管鹏飞)
Chin. Phys. B, 2025, 34 (**3**): 036105. DOI: 10.1088/1674-1056/ada756

Effect of Y element on atomic structure, glass forming ability, and magnetic properties of FeBC alloy

Jin-Hua Xiao(肖晋桦), Da-Wei Ding(丁大伟), Lin Li(李琳), Yi-Tao Sun(孙奕韬), Mao-Zhi Li(李茂枝), and Wei-Hua Wang(汪卫华)
Chin. Phys. B, 2024, 33 (**7**): 076101. DOI: 10.1088/1674-1056/ad3dd4

Structural origin for composition-dependent nearest atomic distance in Cu-Zr metallic glass

Chi Zhang(张驰), Hua-Shan Liu(刘华山), and Hai-Long Peng(彭海龙)
Chin. Phys. B, 2023, 32 (**11**): 116101. DOI: 10.1088/1674-1056/acce99

Spatial correlation of irreversible displacement in oscillatory-sheared metallic glasses

Shiheng Cui(崔世恒), Huashan Liu(刘华山), and Hailong Peng(彭海龙)
Chin. Phys. B, 2022, 31 (**8**): 086108. DOI: 10.1088/1674-1056/ac65f3

Heredity of clusters in the rapidly cooling processes of Al-doped $Zr_{50}Cu_{50}$ melts and its correlation with the glass-forming ability

Dadong Wen(文大东), Yonghe Deng(邓永和), Ming Gao(高明), and Zean Tian(田泽安)
Chin. Phys. B, 2021, 30 (**7**): 076101. DOI: 10.1088/1674-1056/abea93

Optimization of glass-forming ability and synergistic enhancement of strength plasticity in $Cu_{50}Zr_{46}Al_4$ metallic glasses through Ag additions

Dongmei Li(李冬梅)[1], Zhongyi Zhang(张忠一)[1], Bolin Shang(尚博林)[1], Rui Feng(丰睿)[1], Xuefeng Li(李雪枫)[2,†], and Peng Yu(余鹏)[1,‡]

[1] *College of Physics and Electronic Engineering, Chongqing Normal University, Chongqing* 401331, *China*
[2] *Chongqing Key Laboratory of Public Big Data Security Technology, Chongqing College of Mobile Communication, Qijiang* 401420, *China*

(Received 24 March 2025; revised manuscript received 15 April 2025; accepted manuscript online 21 April 2025)

Bulk metallic glasses (BMGs) are typically characterized by high strength and elasticity. However, they generally demonstrate a deficiency in plastic deformation capability at room temperatures. In this work, $Cu_{50-x}Zr_{46}Al_4Ag_x$ ($x = 0$, 1, 2, 3, 4) alloys were prepared by arc melting and copper mold casting to investigate their structure, glass-forming ability, and mechanical properties. The results show that the addition of Ag can increase the parameter of ΔT_x and γ in $Cu_{50}Zr_{46}Al_4$ alloy by 116% and 1.5% respectively, effectively enhancing its thermal stability and glass-forming ability. Compressive fracture tests reveal that the addition of Ag can significantly improve the yield strength, ultimate strength, and plasticity of the $Cu_{50}Zr_{46}Al_4$ alloy. Specifically, with the Ag addition of 1 at.%, the alloy's ultimate strength and plasticity increased by 71.8% and 21 times, respectively. Furthermore, the introduction of Ag can effectively control the free volume content in the $Cu_{50}Zr_{46}Al_4$ alloy, thereby tuning the hardness of the material. This work provides valuable insights into improving the mechanical performance of BMGs through micro-alloying approaches.

Keywords: metallic glasses, glass-forming ability, synergistic enhancement strength-plasticity, Ag addition

PACS: 61.25.Mv, 61.43.Dq, 62.20.F–

DOI: 10.1088/1674-1056/adcea1 **CSTR:** 32038.14.CPB.adcea1

1. Introduction

Metallic glasses, also known as amorphous alloys, typically exhibit higher strength, larger elastic limits, and better corrosion resistance compared to traditional crystalline alloys, making them widely used as structural materials. In recent years, many BMGs with excellent mechanical properties have been developed.[1–3] However, how to further enhance the glass-forming ability (GFA) and optimize the mechanical performance of metallic glasses remains a focus of industry attention. Cu-based BMGs are considered promising structural materials due to their relatively high strength, high thermal stability, and low cost.[4–6] Ternary Cu-based BMGs were first discovered by the Inoue's group in the Cu–Zr–Ti and Cu–Zr–Al alloy systems.[7,8] Subsequently, a series of Cu-based BMGs, such as Cu–Zr–Ag,[9] Cu–Hf–Al,[10] and Cu–Hf–Ti,[11] have been reported. These BMGs generally possess high strength, good GFA, and economical pricing. Among them, Cu–Zr-based BMGs have attracted significant attention due to their simple composition, non-toxicity, lack of precious metal elements, large GFA, and wide composition range.[12–14] The Cu–Zr–Al system, is considered one of the most promising Cu-based system in metallic glass, as it exhibits excellent strength and high GFA.[15,16]

Researches have shown that the addition or substitution of elements can enhance the degree of atomic disorder in BMG alloys, leading to improved GFA.[14–22] Microalloying has been proven to be an effective approach for tuning the various properties of BMGs. For example, Lin *et al*. effectively improved the soft magnetic performance of the $Fe_{40}Cr_{19}Mo_{18}C_{15}B_8$ alloy by adding a small amount of the magnetic P.[23,24] Similarly, Zhang *et al*. enhanced the GFA and thermal stability of Zr–Cu-based metallic glasses by adding Si,[25,26] while Ma *et al*. reported that the addition of carbon can improve the mechanical properties of the $Fe_{80}Si_1P_{10}C_9$ alloy by approximately 40%.[27–29] At the same time, microalloying has a significant effect on the properties of Cu glass. For example, Ma and Pan *et al.* achieved effective regulation of mechanical properties and thermal stability of $Cu_{46}Zr_{45}Al_7$ BMG by adding trace Fe elements.[30–32]

Ag, as a transition metal element, is soft, highly ductile, and possesses excellent electrical and thermal conductivity, which may further improve the thermodynamic properties and GFA of alloys. Additionally, based on the empirical criteria for metallic glass formation,[33] the significant size difference between Ag atoms and Cu, Zr, Al atoms may promote

†Corresponding author. E-mail: 15584202964@163.com
‡Corresponding author. E-mail: pengyu@cqnu.edu.cn

© 2025 Chinese Physical Society and IOP Publishing Ltd. All rights, including for text and data mining, AI training, and similar technologies, are reserved.

the formation of a tightly packed random atomic structure, potentially enhancing the GFA of Cu–Zr-based BMGs through Ag additions. In this study, a series of Cu–Zr–Al–Ag alloys were prepared using $Cu_{50}Zr_{46}Al_4$ as the base alloy and micro-alloying with the transition metal Ag. A systematic investigation was conducted to explore the influence of Ag additions on the structure, GFA, and thermodynamic properties of the $Cu_{50}Zr_{46}Al_4$ BMG system, and its physical mechanism was revealed.

2. Experimental details

2.1. Sample preparation

High-purity (> 99.9 wt%) Cu, Zr, Al, and Ag metallic elements were used as raw materials. The alloy compositions were designed according to the nominal $Cu_{50-x}Zr_{46}Al_4Ag_x$ ($x = 0$, 1, 2, 3, 4 at.%) ratio. The metal elements were melted under an argon atmosphere using an arc melting furnace. The master alloy ingots were remelted five times to ensure compositional and structural homogeneity. The master alloy ingots were then suction cast into copper molds to fabricate cylindrical $Cu_{50-x}Zr_{46}Al_4Ag_x$ ($x = 0$, 1, 2, 3, 4) BMG samples with diameters of 1.5 mm, 3.0 mm, and 5.0 mm using a copper mold water-cooling method.

2.2. Structural and property characterization

The thermal properties of the samples were analyzed using a DSC-8000 differential scanning calorimeter (DSC) and a DTA-8000 thermal analyzer (DTA), both with a heating rate of 20 K/min. X-ray diffraction (XRD) measurements were carried out on the alloy samples using a 6100-type x-ray diffractometer. Hardness testing was performed on the samples using a MHVD-1000AP multi-function Vickers hardness tester. Room-temperature compression tests were conducted on the samples (the length-diameter ratio of the specimen is 2:1) using an RGM-300 universal testing machine at a strain rate of 1×10^{-4} s^{-1}. Finally, the fracture surfaces and morphologies of the alloy samples were characterized using a KYKY-EM6900 scanning electron microscope (SEM).

3. Results and discussion

3.1. Effect of Ag additions on the glass-forming ability of $Cu_{50}Zr_{46}Al_4$

This study employed $Cu_{50}Zr_{46}Al_4$ BMG as the base alloy. By substituting Cu with varying atomic percentages of Ag ($x = 0$, 1, 2, 3, 4) according to predetermined compositions ($Cu_{50-x}Zr_{46}Al_4Ag_x$). Alloy ingots were prepared through repeated arc melting under high-purity argon atmosphere, followed by structural homogenization via copper mold suction casting to produce cylindrical specimens with diameters of 1.5 mm, 3 mm, and 5 mm. Figure 1 presents the XRD patterns of the $Cu_{50-x}Zr_{46}Al_4Ag_x$ alloys. As shown in Fig. 1(a), specimens with diameters of 1.5 mm exhibit a single broad diffuse scattering halo without crystalline diffraction peaks when $x = 0$, 1, 2, 3, indicating that Ag additions up to 3 at.% can preserve the GFA of the $Cu_{50}Zr_{46}Al_4$ matrix. However, at 4-at.% Ag content ($x = 4$), distinct crystalline diffraction peaks emerge, demonstrating partial crystallization and detrimental effects of excessive Ag on GFA. As shown in Fig. 1(b), the intensity of crystalline peaks decreased obviously in both the base alloy and $x = 2$ composition when the specimen diameter increased to 3.0 mm, while prominent crystalline phases are observed in $x = 3$ alloy. Notably, the $x = 1$ alloy maintains a fully amorphous structure characterized by an unbroken diffuse halo, suggesting that 1-at.% Ag addition effectively enhances the GFA of the $Cu_{50}Zr_{46}Al_4$ matrix. As demonstrated in Fig. 1(c), further enlargement of specimen diameter to 5 mm results in crystalline phase formation even in $x = 1$ and $x = 2$ alloys. This confirms that Ag additions lose their GFA-enhancing capability at larger critical dimensions under the present processing conditions.

Investigating thermal properties of the alloys can provides critical insights into the correlation between their thermal stability and variations in GFA. The DSC and DTA curves of the 1.5 mm-diameter $Cu_{50-x}Zr_{46}Al_4Ag_x$ alloys are presented in Figs. 2(a) and 2(b), respectively. Key thermal parameters, including the glass transition temperature (T_g), crystallization temperature (T_x), and melting temperature (T_m) are summarized in Table 1. Compared to the base $Cu_{50}Zr_{46}Al_4$ alloy, the addition of Ag reduced the T_g, T_x, and T_m of the alloys. However, the width of the undercooled liquid region ($\Delta T_x = T_x - T_g$) for all Ag-containing alloys exceeded that of the base alloy. Notably, at 1-at.% Ag content, ΔT_x expanded from 25 K to 54 K, representing a 116% increase compared to the base alloy. The shaded region and dashed lines in Fig. 2(a) highlight the variations in T_g, T_x, and ΔT_x. The enlarged ΔT_x signifies that Ag additions improve the GFA of the $Cu_{50}Zr_{46}Al_4$ system. Furthermore, the γ parameter ($\gamma = T_x/(T_g + T_m)$), a critical indicator of GFA, was analyzed. A higher γ value typically correlates with superior GFA. As shown in Table 1, the γ parameter increased with 1 at.%–2 at.% Ag additions but decreased at 3-at.% Ag. This indicates that moderate Ag doping (1 at.%–2 at.%) enhances the GFA of $Cu_{50}Zr_{46}Al_4$, while excessive Ag (≥3 at.%) degrades it. Figure 2(c) displays the evolution of thermodynamic parameters with Ag content. Both parameters of ΔT_x and γ reach their maxima at 1-at.% Ag, indicating optimal GFA and thermal stability. Beyond this threshold, further Ag additions degrade these properties, confirming that moderate Ag doping (1 at.%–2 at.%) enhances the thermal sta-

bility and the glass-forming ability of $Cu_{50}Zr_{46}Al_4$, while excessive Ag (> 2 at.%) compromises these advantages. In the Cu–Zr–Al–Ag system, the atomic radii of Cu, Zr, Al, and Ag are 0.128 Å, 0.162 Å, 0.143 Å, and 0.144 Å, respectively. The atomic size ratios between Zr/Al (1.118) and Al/Cu (1.117) exceed 12%, creating significant atomic mismatch. The introduction of Ag, with its intermediate atomic size, enhances the packing density in the alloy system. This improved atomic packing strengthens the thermal stability and stabilizes the disordered glassy structure, thereby synergistically enhancing both the glass-forming ability and thermal stabilities in Ag-modified $Cu_{50}Zr_{46}Al_4$ alloys.

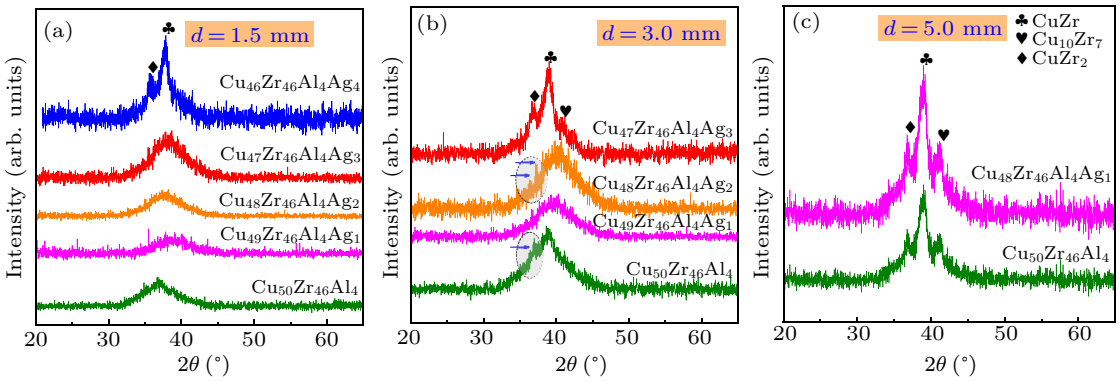


Fig. 1. XRD patterns of $Cu_{50-x}Zr_{46}Al_4Ag_x$ ($x = 0$, 1, 2, 3, 4) alloys with diameters of (a) 1.5 mm, (b) 3.0 mm, and (c) 5.0 mm.

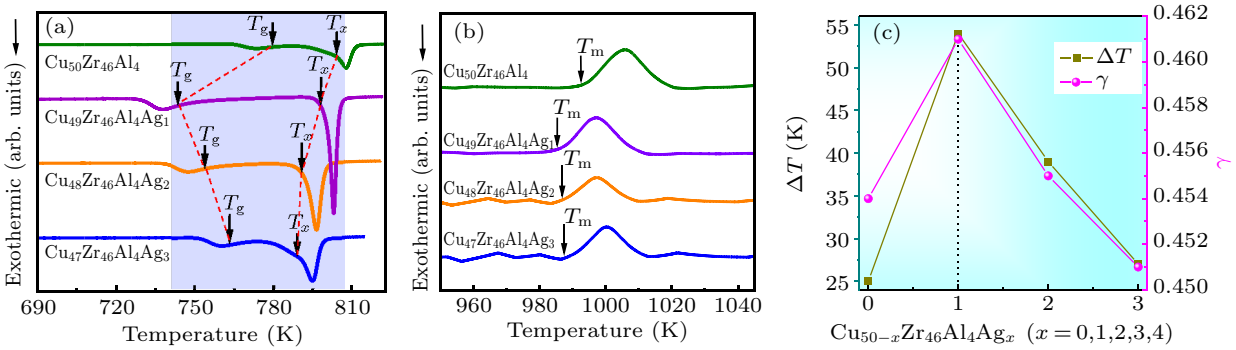


Fig. 2. (a) DSC curves, (b) DTA curves, and (c) thermodynamic parameter variations $Cu_{50-x}Zr_{46}Al_4Ag_x$ ($x = 0$, 1, 2, 3) alloys with a diameter of 1.5 mm at the heating rate of 20 K/min.

Table 1. Thermal parameters of $Cu_{50-x}Zr_{46}A_{l4}Ag_x$ ($x = 0$, 1, 2, 3, 4) alloys with diameter of 1.5 mm.

Alloys (1.5 mm)	T_g (K)	T_x (K)	ΔT_x (K)	T_m (K)	γ
$Cu_{50}Zr_{46}Al_4$	779	804	25	993	0.454
$Cu_{49}Zr_{46}Al_4Ag_1$	743	797	54	985	0.461
$Cu_{48}Zr_{46}Al_4Ag_2$	752	791	39	986	0.455
$Cu_{47}Zr_{46}Al_4Ag_3$	763	790	27	989	0.451

3.2. Effect of Ag additions on the mechanical properties of $Cu_{50}Zr_{46}Al_4$

Figure 3(a) presents the compressive stress–strain curves of 1.5-mm-diameter $Cu_{50-x}Zr_{46}Al_4Ag_x$ alloys tested at room temperature. The corresponding yield strength (σ_y), fracture strength (σ_f), and plastic strain (ε_p) are summarized in Table 2. As shown, the base $Cu_{50}Zr_{46}Al_4$ alloy exhibits negligible yielding and limited plastic deformation ($\varepsilon_p = 0.3\%$). With Ag additions, all modified alloys demonstrate pronounced elastic deformation during the initial loading stage, accompanied by significant improvements in fracture strength and plasticity. Notably, the $Cu_{49}Zr_{46}Al_4Ag_1$ alloy displays remarkable compressive plasticity with a 21-times increase in ε_p (6.6%) compared to the base alloy, alongside a 71.8% enhancement in σ_f (2.13 GPa). Further Ag additions ($x \geq 2$) gradually reduce both σ_f and ε_p, though these values remain superior to $Cu_{50}Zr_{46}Al_4$ alloy. As illustrated in Fig. 3(b), σ_y, σ_f, and ε_p exhibit a synergistic enhancement effect, reaching optimal values at 1-at.% Ag. This demonstrates that trace Ag doping (1 at.%) in $Cu_{50}Zr_{46}Al_4$ BMG simultaneously strengthens the matrix while improving ductility, achieving a balanced strength–plasticity synergy.

The addition of Ag also effectively modulates the Young's modulus and hardness of the $Cu_{50}Zr_{46}Al_4$ alloy. As shown in Fig. 4(a), Ag doping generally enhances the Young's modulus, with the 1-at.% Ag-modified alloy exhibiting the maximum value. Further increases in Ag content leads to a gradual decline in Young's modulus. Figure 4(b) illustrates the Vickers hardness (HV) trends for 1.5 mm and 3.0-mm-diameter $Cu_{50-x}Zr_{46}Al_4Ag_x$ alloys. Notably, the HV of the $Cu_{50-x}Zr_{46}Al_4Ag_x$ system decreases monotonically with increasing Ag content, which can be attributed to the inherently soft nature of Ag atoms, which reduces the overall hardness of the alloy. Additionally, for the same Ag concentrations, in

the 1.5-mm-diameter specimens exhibit lower hardness compared to their 3.0-mm counterparts. This discrepancy arises from the faster cooling rate during the fabrication of smaller-diameter specimens, which introduces higher free volume into the alloy system, thereby softening the material.

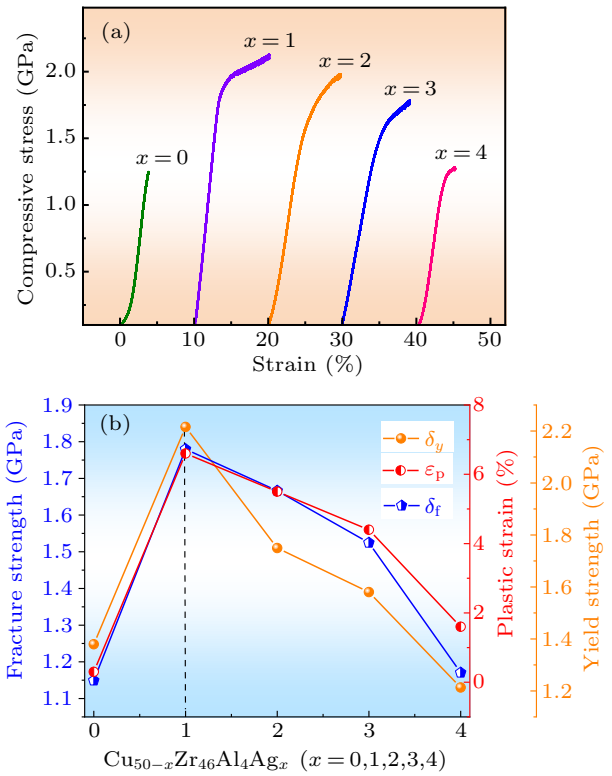


Fig. 3. (a) Stress–strain curves and (b) the statistics of mechanical parameters of $Cu_{50-x}Zr_{46}Al_4Ag_x$ ($x=0$, 1, 2, 3, 4) alloys with a diameter of 1.5 mm at room temperature.

Table 2. Compressive mechanical parameters of $Cu_{50-x}Zr_{46}Al_4Ag_x$ ($x=0$, 1, 2, 3, 4) alloys with a diameter of 1.5 mm at room temperature.

	σ_y (GPa)	σ_f (GPa)	ε_p (%)
$Cu_{50}Zr_{46}Al_4$	–	1.24	0.3
$Cu_{49}Zr_{46}Al_4Ag_1$	1.84	2.13	6.6
$Cu_{48}Zr_{46}Al_4Ag_2$	1.51	1.97	5.5
$Cu_{47}Zr_{46}Al_4Ag_3$	1.39	1.77	4.4
$Cu_{46}Zr_{46}Al_4Ag_4$	1.13	1.27	1.6

Figure 5 compares the fracture surface and lateral morphology of compressed $Cu_{50}Zr_{46}Al_4$ and $Cu_{49}Zr_{46}Al_4Ag_1$ alloys. As shown in Figs. 5(a) and 5(b), the fracture surface of the Ag-doped alloy exhibits more distinct and periodically arranged vein-like patterns compared to the base alloy, consistent with its superior strength and plasticity. Figures 5(c) and 5(d) display the lateral morphologies of the fractured specimens. The $Cu_{49}Zr_{46}Al_4Ag_1$ alloy demonstrates a significantly higher density of shear bands with intricate spatial distribution, reflecting enhanced plastic deformation capability. In contrast, the $Cu_{50}Zr_{46}Al_4$ alloy shows sparse and localized shear bands. This improvement arises from the Ag-induced structural modification: the introduction of Ag atoms increases atomic-level disorder in the Cu–Zr–Al–Ag system (atomic radii: Cu = 0.128 Å, Ag = 0.144 Å), which promotes shear band nucleation and multiplication rather than catastrophic crack propagation. The resulting shear band interaction delays fracture and synergistically improve strength and ductility.

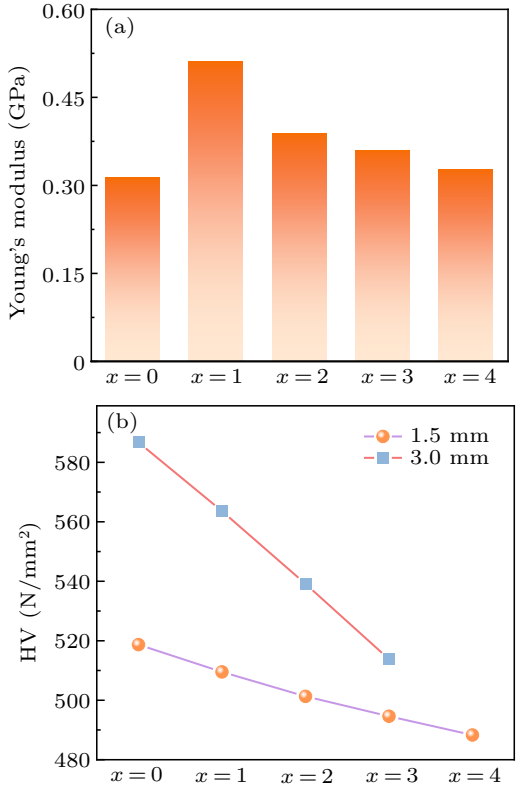


Fig. 4. (a) Young's modulus and (b) HV of $Cu_{50-x}Zr_{46}Al_4Ag_x$ ($x=0$, 1, 2, 3, 4) alloys.

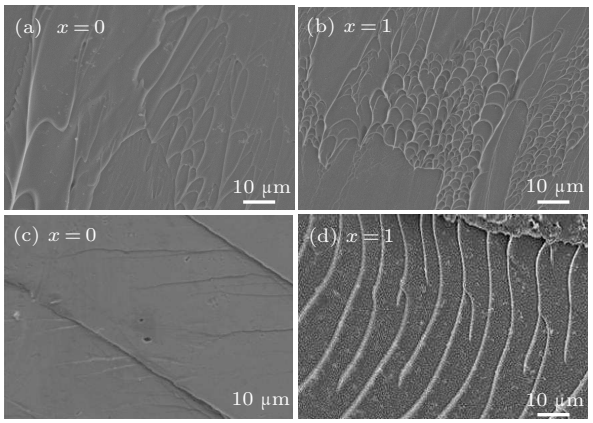


Fig. 5. SEM photographs of [(a)–(b)] the fracture surface and [(c)–(d)] the lateral surface of the $Cu_{50-x}Zr_{46}Al_4Ag_x$ ($x=0$, 1) alloys.

4. Conclusion

This study systematically investigated the effects of Ag doping on the structural, thermal, and mechanical properties of $Cu_{50}Zr_{46}Al_4$ BMG by substituting Cu with Ag at varying atomic ratios ($Cu_{50-x}Zr_{46}Al_4Ag_x$, $x=0$, 1, 2, 3, 4). The alloys were characterized for their thermal stability, GFA, hardness, and compressive stress–strain behavior. Key findings reveal that controlled Ag additions significantly enhance the thermal

stability and GFA of $Cu_{50}Zr_{46}Al_4$. At 1-at.% Ag, the ΔT_x increased by 116% (from 25 K to 54 K), while the γ parameter peaked at 0.461, indicating optimal GFA. Mechanically, the $Cu_{49}Zr_{46}Al_4Ag_1$ achieved exceptional strength–plasticity synergy: compressive σ_f and ε_p reached 2.144 GPa and 6.6%, respectively, representing 71.8% increase in strength and 21 times improvement in plasticity compared to the $Cu_{50}Zr_{46}Al_4$ alloy. Furthermore, Ag doping modulated the elastic and hardness properties of the $Cu_{50}Zr_{46}Al_4$ alloy. Young's modulus initially rose with 1-at.% Ag but declined at higher concentrations, while Vickers hardness decreased monotonically with Ag content due to its intrinsic softness and cooling rate-dependent free volume formation. Fractographic analysis corroborated these trends, with Ag-doped alloys exhibiting refined shear band patterns and enhanced shear band density, directly linked to improved atomic-level disorder and delayed fracture. This work provides critical insights into designing Cu–Zr–Al-based BMGs with balanced GFA and mechanical performance through strategic microalloying, offering a viable pathway to overcome the traditional strength-ductility trade-off in metallic glasses.

Acknowledgements

Project supported by the National Natural Science Foundation of China (Grant Nos. 12404228 and 52371148) and the Science and Technology Research Program of Chongqing Education Commission of China (Grant No. KJQN202200510).

References

[1] Kui H W, Greer A L and Turnbull D 1984 *Appl. Phys. Lett.* **45** 615
[2] Wang W 2013 *Prog. Phys.* **33** 177 (in Chinese)
[3] Liang S Y, Zhu F, Wang Y J, Pineda E, Wad T, Kato H and Qiao J C 2024 *Int. J. Eng. Sci.* **205** 104146
[4] Q Zhang, W Zhang and Inoue 2006 *Acta Mater.* **55** 711
[5] Yu P, Bai H Y, Tang M B and Wang W H 2005 *J. Non-Cryst. Solids* **351** 1328
[6] Yu P, Bai H Y and Wang W H 2006 *J. Mater. Res.* **21** 1674
[7] Inoue A and Zhang W 2002 *Mater. Trans.* **43** 2921
[8] Inoue A, Zhang W, Zhang T and Kurosaka K 2001 *Mater. Trans.* **42** 1149
[9] Zhang Q, Zhang W, Xie G and Inoue A 2007 *Mater. Trans.* **48** 1626
[10] Vincent S, Peshwe D R, Murty B S and Bhatt J 2011 *J. Non-Cryst. Solids* **357** 3495
[11] Inoue A, Zhang W, Zhang T and Kurosaka K 2001 *Acta Mater.* **49** 2645
[12] Eckert J, Das J, Kim K B, Baier F, Tang M B, Wang W H and Zhang Z F 2006 *Intermetallics* **14** 876
[13] Dong C, Wang Q, Qiang J B, Wang Y M, Jiang N, Han G, Li Y H, Wu J and Xia J H 2008 *J. Phys. D: Appl. Phys.* **40** R273
[14] Tan H, LiY and Wang D 2005 *Acta Mater.* **53** 2969
[15] Yu P and Bai H Y 2008 *Mater. Sci. Eng. A* **485** 1
[16] Li D M, Chen L S, Yu P, Ding D and Xia L 2020 *Chin. Phys. Lett.* **37** 086401
[17] Xiao J H, Ding D W, Li L, Sun Y T, Li M Z and Wang W H 2024 *Chin. Phys. B* **33** 076101
[18] Men H, Wang X K, Fu J Y and Chao L M 2006 *Mater. Trans.* **47** 194
[19] Plummer J D and Todd I 2011 *Appl. Phys. Lett.* **98** 021907
[20] Zhang Q, Zhang W, Xie G Q and Inoue A 2008 *Mater. Sci. Eng. B* **148** 97
[21] Louzguine-Luzgin D V, Xie G, Zhang W and Inoue A 2007 *Mater. Sci. Eng. A* **465** 146
[22] Zhang S, Li Q A, Yang Y and Guan P F 2025 *Chin. Phys. B* **34** 036105
[23] Lin T J, Sheu H H, Lee C Y and Lee H B 2021 *J. Alloys Compd.* **867** 159132
[24] Tong X, Zhang Y, Wang Y, Liang X, Zhang K, Zhang Fan, Cai Y, Ke H, Wang G, Shen J and Makino A 2022 *J. Mater. Sci. Technol.* **96** 233
[25] Zhang B, Jia Y, Wang S, Li G, Shan S F, Zhan Z J, Liu R P and Wang W K 2009 *J. Alloys Compd.* **468** 187
[26] Lu Z P and Liu C T 2002 *Acta Mater.* **50** 3501
[27] Kim H S, Lee J C, Kim Y C, Lee S H, Lee B J and Ahn J P 2004 *Acta Mater.* **52** 1525
[28] Song K K, Pauly S and Zhang Y 2011 *Intermetallics* **19** 1394
[29] Ma Y, Xie L, Li Q, Chang C, Li H, Mu B and Ma X 2022 *J. Phys. Chem. Solids* **163** 110596
[30] Park E S and Kim D H 2006 *Acta Mater.* **54** 2597
[31] Pan J, Liu L and Chan K C 2009 *Scr. Mater.* **60** 822
[32] Kim Y C, Lee J C, Cha P R, Ahn J P and Fleury E 2006 *Mater. Sci. Eng. A* **437** 248
[33] Dong B, Zhou S, Li D, Lu C, Guo F, Ni X and Lu Z 2011 *Prog. Nat. Sci.: Mater. Int.* **21** 164